



**HAL**  
open science

# Electrical conductivity of the mantle of Mars from MGS magnetic observations

François Civet, Pascal Tarits

► **To cite this version:**

François Civet, Pascal Tarits. Electrical conductivity of the mantle of Mars from MGS magnetic observations. *Earth Planets and Space*, 2014, 66 (1), pp.article n° 85. 10.1186/1880-5981-66-85 . insu-01118514

**HAL Id: insu-01118514**

**<https://insu.hal.science/insu-01118514>**

Submitted on 13 Oct 2021

**HAL** is a multi-disciplinary open access archive for the deposit and dissemination of scientific research documents, whether they are published or not. The documents may come from teaching and research institutions in France or abroad, or from public or private research centers.

L'archive ouverte pluridisciplinaire **HAL**, est destinée au dépôt et à la diffusion de documents scientifiques de niveau recherche, publiés ou non, émanant des établissements d'enseignement et de recherche français ou étrangers, des laboratoires publics ou privés.



Distributed under a Creative Commons Attribution 4.0 International License

LETTER

Open Access

# Electrical conductivity of the mantle of Mars from MGS magnetic observations

François Civet<sup>1,2\*</sup> and Pascal Tarits<sup>2</sup>

## Abstract

Mars Global Surveyor (MGS) magnetic data were analyzed to obtain the electromagnetically induced response of the Martian mantle. The time-varying part of the MGS magnetic data analysis was obtained by removing a model of the static field. Only night data were selected and binned on a regular grid. The binned time series were processed using a proxy of the transient magnetic field. Two proxies were designed, one based on the MGS data themselves and one built from the Advanced Composition Explorer (ACE) dataset. The internal induced response of the planet was obtained at periods ranging from more than 1 to 200 days. The induced responses were inverted to infer the mantle's electrical conductivity down to about 1,300 km. The comparison of our conductivity profiles with previous theoretical studies confirms an atherm close to the cold boundary of thermal models of the Mars interior. A mantle transition zone was determined between 1,000 and 1,200 km deep.

**Keywords:** Electrical conductivity; Electromagnetic induction; Mars mantle; Mars Global Surveyor; Magnetic field

## Findings

### Introduction

The increase in knowledge about the deep interior of Mars acquired in the past decade still relies on a very limited amount of data. Only a few geochemical, geophysical, and astronomical observations provide reliable constraints on the planet's mantle. Estimates of the Martian mantle composition are derived from geochemical studies of a set of basaltic achondrite meteorites, collectively designated the SNCs (shergottites, nakhlites, and chassignites) (e.g., Dreibus and Wanke 1985; Bertka and Fei 1997; Sanloup et al. 1999). Areodesy observations provide information on mass, mean density, and moment of inertia to build models of the deep interior of Mars (e.g., Khan and Connolly 2008; Rivoldini et al. 2011; Konopliv et al. 2011). All these studies highlight the need for new geophysical data. This study aims to discriminate the thermal profile (hot or cold), to obtain crucial information about the mineralogical assembly (peridotite or pyroxenic), and to determine the mineralogical transition zone of the Martian mantle from those proposed in the literature (Dreibus and

Wanke 1985; Bertka and Fei 1997; Sohl and Spohn 1997; Sanloup et al. 1999; Mocquet and Menvielle 2000).

As no seismic observations are available yet, mantle structures in planet Mars may be directly inferred by studying the observed magnetic field. The most extensive magnetic dataset outside the Earth was obtained during the Mars Global Surveyor (MGS) mission (Acuña et al. 2001). These data are comparable to Earth satellite data in length (several years) and quality, but with a complex time-varying field (Dubinin et al. 2008; Kallio et al. 2008) resulting from the interaction between the solar wind and the environment of the planet. This transient magnetic field induces electric currents in the planet's crust and mantle, which are in turn responsible for an internally induced magnetic field superimposed on the former one. Electromagnetic induction (EI) is therefore a process that gives access to the electric properties of the planet through observation of the transient magnetic field (e.g., Tarits 1994). Mocquet and Menvielle (2000) and Vacher and Verhoeven (2007) demonstrated the sensitivity of conductivity and EI data to different mantle compositions and temperature using the mineralogical assembly proposed by e.g., Dreibus and Wanke 1985 from an analysis of elementary ratios in SNC meteorites. Mocquet and Menvielle (2000) tested two mineralogical compositions,

\*Correspondence: francois.civet@univ-nantes.fr

<sup>1</sup>LPG-Nantes, University of Nantes, 2 rue de la Houssinière, Nantes 44322, France

<sup>2</sup>LDO-IUEM, University of Western Brittany, Plouzané 29280, France

olivine-rich (e.g., Dreibus and Wanke 1985) and pyroxene-rich, of the Mars mantle to obtain profiles of electrical conductivity (Sanloup et al. 1999) and both hot and cold thermal profiles.

#### **Mars magnetic field and the MGS data**

The magnetic dynamo shut down more than 4 Gyrs ago (Hood et al. 2007). Magnetic sources therefore originate from remanent magnetization and exospheric fields. Due to the lack of a main magnetic field of internal origin, Mars does not have a magnetospheric shield. Thus, energetic particles of the solar wind interact directly with particles of the ionopause, creating a highly conductive layer under the satellite, at an altitude of 150 to 200 km on the dayside (Kallio et al. 2008). Moreover, during energetic solar storms, particles of the solar wind can travel through the atmosphere to the planetary surface. They interact with crustal magnetic anomalies, creating mini-magnetospheres (Kallio et al. 2008) and numerous magnetic perturbations on the dayside of the planet.

Mars Global Surveyor measured quasi-continuous time series of the three components of the Martian magnetic field for 8 years in a quasi-circular and polar orbit configuration (Acuña 1999) at a mean altitude of 380 km during the mapping phase period (1999 to 2006). The orbit plane was fixed in local time (2 a.m. to 2 p.m.) during the mapping phase. Datasets were acquired both in planetocentric coordinates ( $X$  toward longitude 0, Airy crater) and in Sun-state system coordinates ( $X$  toward the Sun). The MGS magnetic dataset has an ideal spatial coverage to infer the overall induced response to external electromagnetic forcing. Magnetic dataset was acquired at a nominal sampling rate of 32 samples per second and averaged to 0.75, 1.5, or 3.0 s according to the memory allocation. The memory allocation were determine with respect to the Mars-Earth distance (see Figure 1) with a dynamic accuracy from 0.002 to 32.768 nT with respect to the amplitude of the field. EI analysis is based on the study of the time-varying part of the recorded magnetic field. The first step in the data processing was therefore to reduce the magnetic field from the static crustal field. The latter was removed using the equivalent dipole model calculated by Langlais et al. 2004 for each position of the spacecraft. Thus, from now on, the magnetic field refers to the MGS field minus the static crustal field.

The purpose of EI analysis is to determine the induced part of the magnetic field carrying information about the electrical conductivity of the Mars mantle. With satellite measurements, the magnetometer samples both the time-varying and the spatial geometry of the transient field simultaneously. The discontinuous sampling impacts the recovery of the EI response functions. The sampling of MGS magnetic data is presented in Figure 1 expressed in daily percentage of available data compared

to a continuous nominal maximum sampling. It can be seen in Figure 1 that the sampling rate varies from 100% to 25% with respect to the distance Earth-Mars with a 2-year periodicity. The MGS magnetic mission was not designed to perform electromagnetic induction studies, and the dataset contains gaps from a few seconds to several days mainly during communication with the Earth, due to the presence of high-gain antennae close to the magnetometers, or during orbit adjustments (Acuña et al. 2001).

The MGS data were analyzed using the technique proposed by Civet and Tarits (2013) which combines satellite data binning on a regular grid and a time-series proxy of the time-varying field (see Additional file 1). The spatial grid on which the data were binned was defined by making a compromise between the number of samples per mesh and the spatial resolution. The grid was defined by two polar caps of 30° latitudinal extension, 12 high-latitude meshes of 30° by 60°, and 144 mid-latitude and equatorial meshes of 15° by 15°. This method involves the generation of additional gaps in the time series. Moreover, on the dayside, the satellite is above the ionopause (Kallio et al. 2008) precluding the separation between the external inducing and internal induced magnetic field. Thus, only night-time data were selected (Acuña et al. 2001). Moreover, crustal magnetic models are calculated using only nightside data (e.g., Langlais et al. 2004) to limit the external contamination in magnetic data. The selection of nightside data increased the number of gaps in the data.

#### **MGS and ACE proxies**

Completing magnetic time series with a proxy of the time-varying magnetic activity in a planet environment is necessary to compute the time spectra of the magnetic field components and thus determine the EI responses. On Earth, several indices are defined to characterize the source field activity (e.g., Menvielle and Marchaudon 2007). In global EI studies, the Dst index provides the required information for the magnetospheric activity. As a result, using the Dst index as a proxy means considering that the source field is dominated by the ring current effect which is a reasonable approximation on Earth (e.g., Kuvshinov and Olsen 2006). The Dst index is in fact a synthesis of data from several geomagnetic observatories close to the magnetic equator. Civet and Tarits (2013) derived a proxy representative of the temporal variability of the external source directly from satellite data, averaging components of the magnetic field over half orbit. This method called 'self-proxy method' led to similar results for the Earth's mantle conductivity. We applied this method to MGS. In practice, each magnetic field component was averaged every half-orbit containing more than 500 data points. The data were then re-interpolated to obtain a regular hourly time series. For gaps shorter than 5 h, a

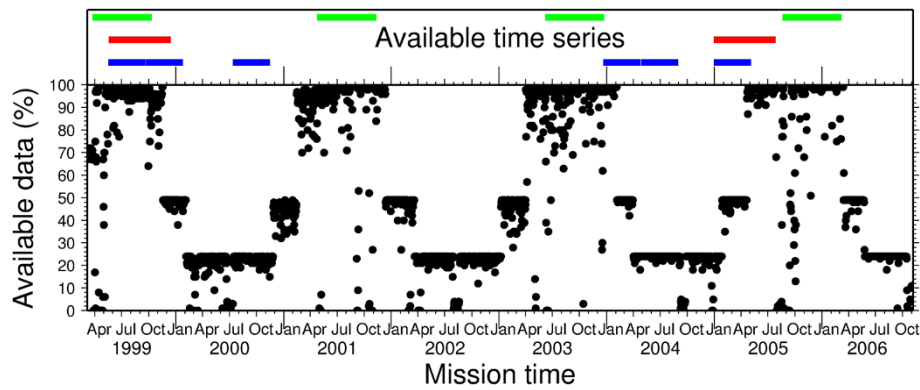


**Figure 1** Daily sampling of magnetic data of MGS during the mapping phase. Expressed in percentage of available data taking into account a continuous nominal maximum sampling. The upper part presents the 12 time series used for our calculations using both proxies: proxy-MGS-1, 6 time series of 125 days (blue); proxy-MGS-2, 2 time series of 210 days (red); proxy-ACE, 4 time series of 200 days.

Lagrangian polynomial interpolation was applied. With these criteria (half orbit of more than 500 samples and gaps less than 4 to 5 h) six continuous time windows of 125 days and two time windows of 210 days were obtained (Figure 1). These proxies were noted proxy-MGS-1 for the 125-day windows and proxy-MGS-2 for the 210-day windows. The self-proxy technique was tested to represent the temporal variability of the EM source on Earth using Ørsted magnetic data (Neubert et al. 2001). The results were in agreement with previous studies (Olsen 1999a; Semenov and Jozwiak 1999; Kuvshinov and Olsen 2006; Velimsky 2010; Civet and Tarits 2013); more information is available in Additional file 1.

The only other dataset available and usable during the MGS mission is the solar wind set of parameters, which has been continuously recorded by the Advanced Composition Explorer (ACE) satellite located at the L1 Lagrange point of the Earth-Sun system since 1997 (Stone et al. 1998). Vennerstrom (2003) showed that the interplanetary magnetic field (IMF) deduced from the ACE dataset may be extrapolated to the Mars region when Mars and Earth are close to the same arm of the Parker spiral (Parker 1958). In contrast with Earth's ionized environment, Mars magnetic activity is a fairly direct function of the IMF (Vennerstrom 2003), and we assumed that the time-varying magnetic field recorded by MGS was approximately proportional to the fluctuations of the IMF. Following Vennerstrom (2003), the ACE time series was time-shifted to the Mars position assuming a constant velocity of  $V_m = 400 \text{ km s}^{-1}$  for the particles carrying the IMF (see Additional file 1 for details). Four periods of 200 days were determined (Figure 1) when the time shift between ACE and Mars was shorter than 4 days. These time series corresponded to time spans when the sampling rate of the MGS data was maximal. This proxy was called proxy-ACE.

Figure 2 shows four simultaneous time series of the time-shifted ACE data for the three magnetic components in heliocentric coordinates, which are compared to the MGS Sun-state dataset  $B_x$ ,  $B_y$ , and  $B_z$  (proxy-SU). The Sun-state coordinate system is defined by the following characteristics: the  $X$ -axis lies along the instantaneous Mars-Sun vector and is positive toward the Sun, the  $Y$ -axis is the vector cross product of  $X$ , and  $Z$  is the vector parallel to the northward (upward) normal of the orbit plane of Mars. The dataset was first averaged to obtain daily values and remove shorter periods in the signals. Linear (Pearson test) and non-parametric (Kendall and Spearman) correlation coefficients (Press 2007) were calculated between the proxy-ACE and proxy-SU time series (see Additional file 1 for details). We hoped to find a satisfying correlation for at least one component of the magnetic field in order to define a second proxy of the external variability, as predicted by Vennerstrom (2003). Only the  $B_y$  component was significantly correlated. Correlation coefficients were greater than 50% for all sections (see Additional file 1). This level of correlation is remarkable given the strong assumptions that were used to extrapolate the IMF near the Mars environment. For short time spans (less than a day), the correlation was weaker probably because of a draping phenomena close to the planetary bow shock which induces tension and elongation of magnetic field lines. The constant velocity hypothesis is also a strong *a priori* for the temporal resolution of high-frequency phenomena. The significant correlation between the  $B_y$  components of proxy-MGS and proxy-ACE led us to select this vectorial component as proxies for subsequent analyses.

#### El responses and inversion

The methodology proposed by Civet and Tarits (2013) and summarized in Additional file 1 was applied using two

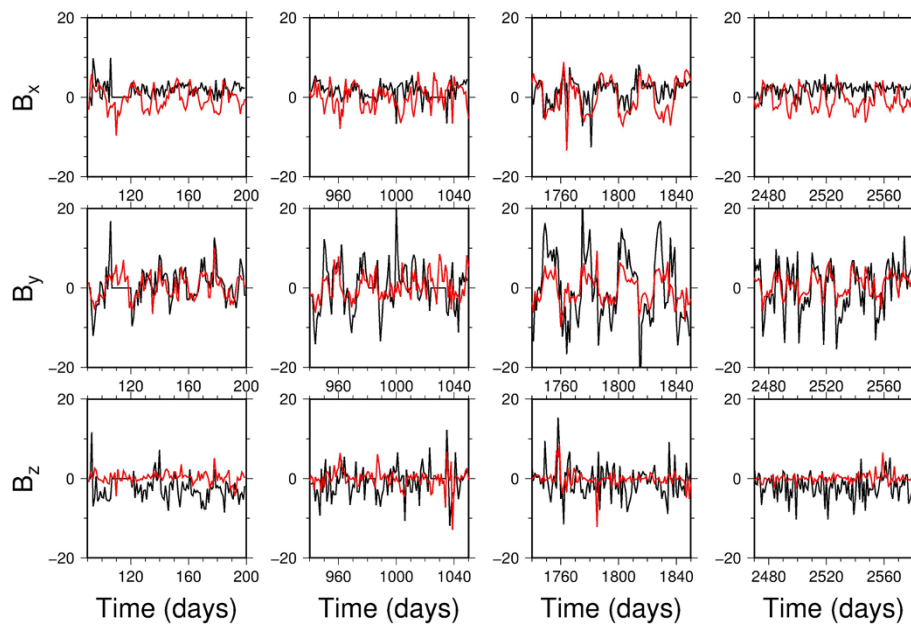


**Figure 2** Four time series of time-shifted IMF compared to MGS measurements. Proxy-SU (black) and proxy-ACE (red) for the three components of the magnetic field (in Sun-state coordinates).

different proxies representative of the temporal variability of the EM source. Three periods of time series were obtained denoted proxy-MGS-1 (six time series of 125 days), proxy-MGS-2 (two time series of 210 days) and proxy-ACE (four time series of 200 days). The spherical harmonic expansion (SH) of the internal and external potentials of the observed MGS magnetic field in the frequency domain was calculated (see Additional file 1 for details). The SH expansion was limited to the longest wavelengths (SH degrees up to  $l = 3$ ), representative of the spatial resolution of the grid. Given the low signal-to-noise ratio (SNR), some of the SH coefficients were not physical. For some specific periods, degree, and order, internal potentials were larger than the external ones. Hence, SH coefficients with values larger than the physically acceptable values were removed (maximum values of the induced/inducing =  $\beta/\alpha$  ratio are 0.5 for  $l = 1$ , 0.66 for  $l = 2$ , and 0.75 for  $l = 3$  for perfect conductive body). Examples of the remaining magnetic external  $\alpha_l^m$  and internal  $\beta_l^m$  potentials at SH degree  $l$  and order  $m$  are synthesized in the form of a spectrogram in Figure 3 for two sets of data using proxy-MGS-2 (210 days) and proxy-ACE (200 days). The energy of SH coefficients  $\alpha_l^m$  and  $\beta_l^m$  was calculated by  $l * |\alpha_l^m|^2$  and  $(l + 1) * |\beta_l^m|^2$ , respectively. For both datasets, the energy was stronger for periods greater than 2 days. There was a dominant amplitude in the external potential  $\alpha_l^m$  at SH degrees 1 to 3 and order 0 for both proxy-MGS and proxy-ACE with a maximum for  $l = 2$ . At present, we cannot confirm the physical process responsible for such a geometry.

For a spherically symmetric body, the EI response to a source of given geometry is necessarily an internal field of the same geometry. Hence, internal SH terms at degrees and orders different from the dominant source terms could reflect the effect of strong mantle heterogeneities (e.g., Olsen 1999b; Tarits et al. 2010). This signal could also be a bias from the analysis in the process of separating the internal from the external field. It is still difficult to quantify the SNR in the data processing, and additional investigations are needed to clarify the origin of these heterogeneous internal SH coefficients.

Considering Mars a spherically symmetric body, for a given conductivity profile, a forward calculation at a given frequency  $\omega$  of the internal induction process for a unitary source potential of strength 1 and SH geometry  $l$ ,  $m$  provides the model's response  $Q_l$ . This value is also equal to the ratio of the observed magnetic SH potential coefficients  $\beta_l^m/\alpha_l^m$  (see Figure 3 and Additional file 1). Multiplying  $Q_l$  by the observed external potential  $\alpha_l^m(\omega)$  gives the theoretical internal induced potential  $\beta_l^m$  at the same frequency to be compared with the observed  $\beta_l^m$ . We applied the 1-D inversion procedure from Civet and Tarits (2013) to obtain the conductivity model that minimizes the misfit between the observed and theoretical  $\beta$  values.

Inversions were carried out for all three SHs,  $l = 1$  to 3,  $m = 0$ , all periods, and all windows for a given proxy model. A large number of inversions with various parameterizations of the Mars mantle were run, varying the number of layers and starting conductivity values. The different acceptable SH coefficients from the

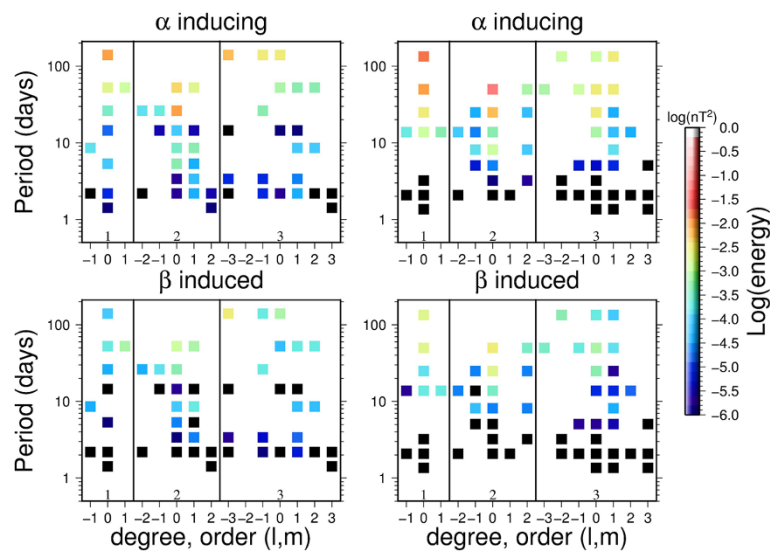


**Figure 3** Spectrograms of external (upper part) and internal (lower part) SH magnetic potential coefficients  $\alpha_l^m$  and  $\beta_l^m$ , respectively. Each panel presents the spectrum obtained for the two proxies, proxy-MGS-2 (left) and proxy-ACE (right). The values are presented in logarithm of energy as a function of degree and order (abscissa) and period in days (ordinate).

whole dataset were tested individually. The values for the 125-day series of MGS and 200-day series of ACE did not seem to provide any quantitative information, probably because of the very low SNR (they all led to a uniform half-space after inversion). Only the SH coefficients obtained using proxy-MGS-2 (210 days long) were accurate enough to provide information on the conductivity, so the final inversion was run on these coefficients only. Results presented in the following refer to this dataset.

We present a model with nine layers. Each layer is 180 km thick so the model encompasses the mantle from Mars surface to its core mantle boundary assumed to be close to 1,600 km in depth (Rivoldini et al. 2011). The core conductivity was set constant and equal to a large value ( $500 \text{ S m}^{-1}$ ). The depth of this boundary was tested even for non-realistic values to infer its influence on results. A very weak influence on models was observed. In fact, below 1,300-km depth, the models were no longer sensitive to data. Models with nine layers of 180 km were calculated, which appeared to be a reasonable compromise between a limited number of parameters, the depth resolution, and the maximum depth of penetration for the data used. Figure 4 shows our preferred model using the SH coefficients restricted to the acceptable set. During the inversion process, all the calculated models were consistent with each other, meaning that a strong geophysical signal was embedded in the SH coefficients, even when considering the complete dataset. A sensitivity analysis was run on these models. The conductivity in each layer was varied to observe the change in the

misfit value. In all models, changing the conductivity values by approximately 0.5 log unit between 0 and 1,300 km increased the misfit by approximately 100% (red shaded area in Figure 4). Below 1,300 km, the data were insensitive to the conductivity structure. Some resulting fits are presented in Additional file 1. The differences between the data and model responses were small for the modulus of the complex coefficient  $\beta$  whereas the phase was poorly

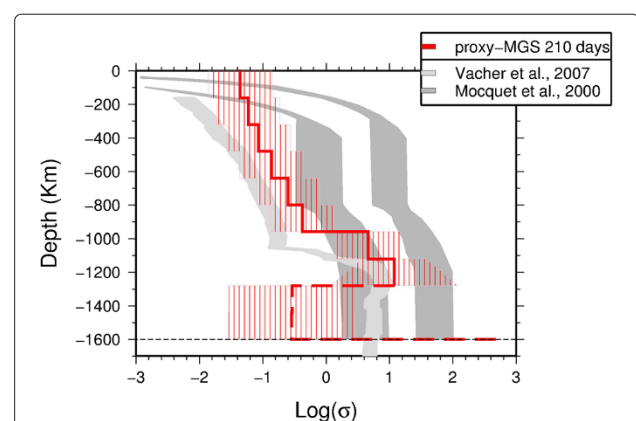


**Figure 4** Preferred conductivity profile. Using only physical SH coefficients for the two time series of 210 days of proxy-MGS. The shaded area denotes the domain of acceptable values determined from the sensitivity analysis. Below 1,300-km depth, data are insensitive to conductivity structure (dashed line). Dark gray areas denote the range of theoretical conductivity models obtained by Mocquet and Menvielle (2000), while light gray area denotes the model constructed by Vacher and Verhoeven (2007).

resolved. It seems that only the modulus is robustly determined while the phase is significantly biased by the large gaps in the data despite the proxies. This is in contrast to the results obtained by Civet and Tarits (2013) on Earth data and outlines the importance of data continuity and/or the quality of proxies in induction studies.

Figure 4 shows an inverted model of electrical conductivity considering only acceptable values of SH coefficients. There is an increase in electrical conductivity from approximately 0 to 1,200 km followed by a rapid jump at approximately 1,000 to 1,200 km. This observation is very stable in the models, even if the depth of the core mantle boundary is changed to more realistic values. The resulting profile appears intermediate between existing models (Mocquet and Menvielle 2000; Vacher and Verhoeven 2007). Moreover, according to mineralogy models for the Mars mantle (Bertka and Fei 1997), the olivine/wadsleyite phase transition should occur in the depth range where a rapid increase in conductivity values is observed.

## Discussion and conclusion

The theoretical studies on the interior electrical conductivity of Mars by Mocquet and Menvielle (2000) and Vacher and Verhoeven (2007) have shown how conductivity values vary with key parameters of the mantle, namely temperature, composition, and iron content. All these parameters are still not well constrained by the available geochemical and geophysical data. When our best models in Figure 4 are compared with the theoretical conductivity models obtained by Mocquet and Menvielle (2000) and Vacher and Verhoeven (2007) based on various mantle compositions and temperature, we observe that our conductivity profiles are clearly on the resistive (cold) boundary of the series of models calculated by Mocquet and Menvielle (2000). Moreover, the prediction of Vacher and Verhoeven (2007), taking into account the effect of a transition zone in the Mars mantle, is confirmed by our findings. This result suggests that the mineral physics approach developed by these authors is acceptable for Mars and could be used to model the mantle composition. The comparison is very encouraging for pursuing studies to improve the quality of the Martian EI response and obtain conductivity models as constrained as possible. Vacher and Verhoeven (2007), Khan and Connolly (2008), Rivoldini et al. (2011), among others clearly demonstrated that the best deep interior models are derived from multi-parameter joint inversion and that the error bars on the geophysical parameters are critical to estimate precisely the various components of the Mars mantle.

The determination of the geometry of the dominant source field on the nightside of the planet suggests another direction of investigation. The dominant terms in the SH of the external magnetic field seem approximately axis-

symmetric with a maximum for  $l = 2$  and  $m = 0$ . The source field might be related to the ion precipitation close to the polar caps (Dieval and Kallio 2012). These models would help to explain our external field model at the period considered (more than 1 day). Further investigations of the MGS data are also required to investigate the field at short periods.

## Additional file

**Additional file 1: Supplementary material.**

## Competing interests

The authors declare that they have no competing interests.

## Authors' contributions

FC carried out the treatment of MGS magnetic data from raw measurement to characterization of electrical conductivity profiles under the supervision of PT during his PhD. Both authors read and approved the final manuscript.

## Acknowledgements

This work was supported by a grant from the French Ministry of Research and from CNRS-INSU (program PNP). We thank the Centre National d'Études Spatiales (CNES). The MGS MAG/ER dataset was obtained from the Planetary Data System (PDS). We are grateful to the anonymous reviewers for their help in improving this article. We also thank Benoit Langlais and Antoine Mocquet for their useful advices.

Received: 7 May 2014 Accepted: 11 July 2014

Published: 4 August 2014

## References

- Acuña MH, Connerney JEP, Ness NF, Lin RP, Mitchell D, Carlson CW, McFadden J, Anderson KA, Reme H, Mazelle C, Vignes D, Wasilewski P, Cloutier P (1999) Global distribution of crustal magnetization discovered by the Mars Global Surveyor MAG/ER experiment. *Science* 284:790–793
- Acuña MH, Connerney JEP, Wasilewski P, Lin RP, Mitchell D, Anderson KA, Carlson CW, McFadden J, Rème H, Mazelle C, Vignes D, Bauer SJ, Cloutier P, Ness NF (2001) Magnetic field of Mars: summary of results from the aerobraking and mapping orbits. *J Geophys Res* 106(E10):23403–23417
- Bertka CM, Fei Y (1997) Mineralogy of the martian interior up to core-mantle boundary pressures. *J Geophys Res* 102(B3):5251–5264
- Civet F, Tarits P (2013) Analysis of magnetic satellite data to infer the mantle electrical conductivity of telluric planets in the solar system. *Planet Space Sci* 84:102–111
- Dreibus G, Wanke H (1985) Mars, a volatile-rich planet. *Meteoritics* 20:367–381
- Dubin E, Fraenz M, Woch J, Winnigham J, Frahm R, Lundin R, Barabash S (2008) Suprathermal electron fluxes on the nightside of Mars: ASPERA-3 observations. *Planet Space Sci* 56(6):846–851
- Dieval C, Kallio E (2012) Hybrid simulations of the proton precipitation patterns onto the upper atmosphere of Mars. *Earth Planets Space* 64:121–134
- Hood L, Richmond N, Harrison K, Lillis R (2007) East-west trending magnetic anomalies in the southern hemisphere of Mars: modeling analysis and interpretation. *Icarus* 191(1):113–131
- Kallio E, Frahm R, Futaana Y, Fedorov A, Janhunen P (2008) Morphology of the magnetic field near Mars and the role of the magnetic crustal anomalies: dayside region. *Planet Space Sci* 56(6):852–855
- Kuvshinov A, Olsen N (2006) A global model of mantle conductivity derived from 5 years of CHAMP, Ørsted, and SAC-C magnetic data. *Geophys Res Lett* 33:18301
- Khan A, Connolly JaD (2008) Constraining the composition and thermal state of Mars from inversion of geophysical data. *J Geophys Res (Planets)* 113(E07003):10.1029/2007JE002996
- Konopliv AS, Asmar SW, Folkner WM, Karatekin O, Nunes DC, Smrekar SE, Yoder CF, Zuber MT (2011) Mars high resolution gravity fields from MRO, Mars seasonal gravity, and other dynamical parameters. *Icarus* 211(1):401–428

- Langlais B, Purucker ME, Mandéa M (2004) Crustal magnetic field of Mars. *J Geophys Res Planets* 109(E2008):10.1029/2003JE002048
- Mocquet A, Menvielle M (2000) Complementarity of seismological and electromagnetic sounding methods for constraining the structure of the martian mantle. *Planet Space Sci* 48:1249–1260
- Menvielle M, Marchaudon A (2007) Geomagnetic indices in solar-terrestrial physics and space weather. chap. 5.1, vol. 344. In: *Space weather*. Springer Netherlands, pp 277–288
- Neubert T, Mandéa M, Hulot G, Von Frese R, Primdahl F, Jørgensen JL, Friis-Christensen E, Stauning P, Olsen N, Risbo T (2001) Ørsted satellite captures high-precision geomagnetic field data. *EOS Trans* 82:81–88
- Olsen N (1999) Long-period (30 days-1 year) electromagnetic sounding and the electrical conductivity of the lower mantle beneath Europe. *Geophys J Int* 138(1):179–187
- Olsen, N (1999) Induction studies with satellite data. *Surv Geophys* 20(3):309–340
- Parker EN (1958) Dynamics of the interplanetary gas and magnetic fields. *Astrophys J* 128:664–676
- Press W (2007) Numerical recipes: the art of scientific computing. Linear correlation & Nonparametric or rank correlation. Chap. 14.5–14.6. London: Cambridge University Press. 745–754
- Rivoldini A, Van Hoolst T, Verhoeven O, Mocquet A, Dehant V (2011) Geodesy constraints on the interior structure and composition of Mars. *Icarus* 213:451–472
- Sanloup C, Jambon A, Gillet P (1999) A simple chondritic model of Mars. *Phys Earth Planet Int* 112(1–2):43–54
- Semenov V, Jozwiak W (1999) Model of the geoelectrical structure of the mid- and lower mantle in the Europe–Asia region. *Geophys J Int* 138(2):549–552
- Sohl F, Spohn T (1997) The interior structure of Mars: implications from SNC meteorites. *J Geophys Res* 102:1613–1636
- Stone E, Frandsen A, Mewaldt R, Christian E, Margolies D, Ormes J, Snow F (1998) The advanced composition explorer. *Space Sci Rev* 86:1–22
- Tarits P (1994) Electromagnetic studies of global geodynamic processes. *Surv Geophys* 15:209–238
- Tarits P, Mandéa M, Suetsugu D, Bina C, Inoue T, Wiens D, Jellinek M (2010) The heterogeneous electrical conductivity structure of the lower mantle. *Phys Earth Planet Int* 183:115–125
- Vacher P, Verhoeven O (2007) Modelling the electrical conductivity of iron-rich minerals for planetary applications. *Planet Space Sci* 55(4):455–466
- Velimsky J (2010) Electrical conductivity in the lower mantle: constraints from CHAMP satellite data by time-domain EM induction modelling. *Phys Earth Planet Int* 180:111–117
- Vennerstrom S, Olsen N, Purucker M, Acuña MH, Cain JC (2003) The magnetic field in the pile-up region at Mars, and its variation with the solar wind. *Geophys Res Lett* 30:1369–1372

doi:10.1186/1880-5981-66-85

**Cite this article as:** Civet and Tarits: **Electrical conductivity of the mantle of Mars from MGS magnetic observations.** *Earth, Planets and Space* 2014 **66**:85.

**Submit your manuscript to a SpringerOpen<sup>®</sup> journal and benefit from:**

- Convenient online submission
- Rigorous peer review
- Immediate publication on acceptance
- Open access: articles freely available online
- High visibility within the field
- Retaining the copyright to your article

Submit your next manuscript at ► [springeropen.com](http://springeropen.com)